
Oxygen quenching in LAB based liquid scintillator and nitrogen bubbling model ^{*}

XIAO Hua-Lin ¹ DENG Jin-Shan

College of Nuclear Science and Technology, Beijing Normal University, Beijing 100875, PR China

Abstract The oxygen quenching effect in Linear Alkyl Benzene (LAB) based liquid scintillator (LAB as the solvent, 3 g/L 2, 5 diphenyloxazole (PPO) as the fluor and 15 mg/L *p*-bis-(*o*-methylstyryl)-benzene (bis-MSB) as the λ -shifter) is studied by measuring the light yield as the function of the nitrogen bubbling time. It is shown that the light yield of the fully purged liquid scintillator is increased by 11% at the room temperature and the room atmosphere pressure. A simple nitrogen bubbling model is proposed to describe the relationship between the relative light yield (oxygen quenching factor) and the bubbling time.

Key words Linear Alkyl Benzene, oxygen quenching, nitrogen bubbling, resolution smearing

PACS 29.40.Mc

1 Introduction

It has been shown experimentally and theoretically that the presence of oxygen in the liquid scintillator (LS) can lower the light yield, modify the fluorescence pulse shape, shorten the attenuation length and decrease the positron annihilation lifetime^[1, 2, 3]. For most aromatic molecules, the quenching of the electronically singlet state (S_1) leads to the formation of triplet state (T_1). The oxygen molecule is somewhat special. Its ground state is a triplet and the next state is a singlet lying about 0.98 eV over the ground state^[4]; Oxygen molecules in aromatic molecules can absorb the energy of singlet state of aromatic molecules, and make the spin allowed transition to the triplet state. This decreases the fluorescence. Such a transition only occurs in aromatic molecules which have a energy gap of $S_1 - T_1$ greater than 0.98 eV. Most of aromatic molecules meet this requirement. In most experiments, the dissolution of oxygen into LS is undesirable. Since this brings uncertainties to the experiments. Hence, the oxygen quenching effect should be well studied and determined.

Usually, there are three ways to eliminate the dissolved oxygen from solutions: 1) the vacuum distillation; 2) the ultrasonic^[5]; 3) the nitrogen(or argon) bubbling^[2]. In neutrino experiments, large quantity of liquid scintillator is required. The most economical

and practicable way to eliminate oxygen in LS is the nitrogen (or argon) bubbling.

Linear alkyl benzene (LAB), which is composed of a linear alkyl chain of 10-13 carbon atoms attached to a benzene ring, is a low cost product of petrochemical industry and is often used as the material of detergent. Its aromatic structure makes it be useful as a scintillator solvents inherently. It has many appealing properties, including the high flash point (130°C), the low toxicity, the high light yield and excellent transparency^[6]. LAB based liquid scintillator will serve as the antineutrino target in the Daya Bay neutrino experiment^[7].

In this work, we measured the effect of oxygen on the light yield of LAB LS, and built a nitrogen bubbling model to describe the relationship between relative light yield (the oxygen quenching factor) and the nitrogen bubbling time. Parameters in the model were determined by our experimental data.

2 Nitrogen bubbling model

When LS is exposed to the air, oxygen molecules dissolved in the LS exchanges with those in the air. This process is in dynamical equilibrium. It is reasonable to assume that the oxygen dissolved in the un-bubbled LS is saturated due to its long time contact with the air. This means that the number of

^{*} Supported by Nation Natural Science Foundation of China (211202037)

1) E-mail: xiaohl@mail.bnu.edu.cn

oxygen molecules dissolving into the LS is equal to those escaping from the LS. When LS is flushed with nitrogen, the oxygen partial pressure in the nitrogen bubble, which presents in LS, can be thought to be zero. Therefore, oxygen molecules will escape from LS and enter the nitrogen bubbles. The dissolution of oxygen molecules into the LS can be ignored in the interface of nitrogen and LS. Since that the oxygen molecules diffusion rate into LS is much higher than the oxygen escaping rate, which denotes that oxygen molecules are uniformly distributed in LS; It is reasonable to assume that the oxygen escaping rate is proportional to the contact area of bubbles with LS and the oxygen partial pressure in LS which is proportional to the oxygen concentration. Then, the equation describing the variation of the oxygen molecule number in LS, dN/dt , is given by

$$\frac{dN}{dt} = -k_e[Q]S, \quad (1)$$

where $[Q]$ is the oxygen concentration dissolved in LS; k_e and S are the oxygen escaping rate and nitrogen–LS contact area, respectively. The oxygen concentration can be expressed as the following:

$$[Q] = \frac{N}{V_s}, \quad (2)$$

where N and V_s are the oxygen molecule number in LS and the LS volume, respectively. Hence, Eq. (1) can be rewritten as

$$\frac{dN}{dt} = -\frac{k_e N}{V_s} S. \quad (3)$$

Then, the variation of the oxygen molecule number in LS is

$$\frac{dN}{N} = -\frac{k_e S}{V_s} dt. \quad (4)$$

Eq. (4) can be written in the integration form:

$$N = N_0 \exp\left(-\frac{k_e S}{V_s} t\right), \quad (5)$$

where N_0 is the oxygen molecule number in LS without bubbling.

At low concentration, the quenching of fluorescence by a quencher in solution can be described by the well-known Stern-Volmer relationship,

$$\frac{I_0}{I} = 1 + k_Q[Q], \quad (6)$$

where I_0 is the intensity or rate of fluorescence without a quencher present, I is the intensity or the rate of fluorescence with a quencher, $[Q]$ is the quencher concentration dissolved in LS, and k_Q is quenching constant.

Hence, the relative light yield as the function of the bubbling time is given by

$$\frac{I_0}{I} = 1 + \frac{k_Q N_0}{V_s} \exp\left(-\frac{k_e S}{V_s} t\right). \quad (7)$$

Note that N_0/V_s is the saturated concentration of oxygen which is dependent of temperature and atmospheric pressure; At fixed temperature and atmospheric pressure, N_0/V_s is a constant. Denote the $k_Q N_0/V_s$ item by a constant A . Then, Eq. (7) turns to be

$$\frac{I_0}{I} = 1 + A \exp\left(-\frac{k_e S}{V_s} t\right). \quad (8)$$

The oxygen quenching factor, f_Q , is defined as the light yield of LS with oxygen to that without oxygen, i.e. I/I_0 . Eq. (8) can be expressed in the form of f_Q ,

$$f_Q = 1/(1 + A \exp(-\frac{k_e S}{V_s} t)). \quad (9)$$

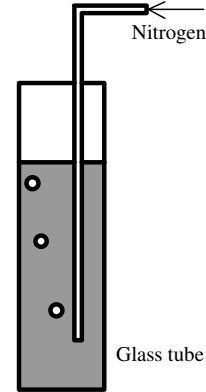


Fig. 1. Bubbling setup

The bubbling setup can be illustrated by the simplified plot in Fig. 1. The nitrogen–LS contact area consists of two parts: the area of the nitrogen bubble surface and the contact surface area of liquid level, i.e.

$$S = nS_b + S_l, \quad (10)$$

where n is the average number of nitrogen bubble present in the LS. S_b and S_l are the average surface area of bubbles and the area of the liquid level, respectively. Then, Eq. (9) can be rewritten as

$$f_Q = 1/(1 + A \exp(-k_e(nS_b + S_l)t/V_s)). \quad (11)$$

The parameters A and k_e are constants depending on the temperature and pressure for specific LS. In the following sections we will evaluate A and k_e for LAB LS at the room temperature and the atmospheric pressure experimentally.

3 Experiment

In order to observe the light output variation due to the oxygen quenching, sets of samples of LS (LAB as the solvent, 3 g/L PPO as the fluor and 15 mg/L bis-MSB as the wavelength shifter) were bubbled with different time. Fig. 1 shows the bubbling setup. Six sets of LS samples (50 ml for each sample) were used. One set of samples was not bubbled, and the other five were bubbled with high purity nitrogen for 5 min (200 ml), 12.5 min (500 ml), 18.7 min (750 ml), 25 min (1000 ml) and 31.25 min (1250 ml), respectively (the numbers in the brackets are the nitrogen volumes). Nitrogen flow rate was precisely controlled at 40 ml/min by a flowmeter. The bubbles present in LS can be thought to be spherical. The bubble number appears in the tube can be easily counted and the diameters of bubbles can be measured with rulers. In our condition, 4 bubbles, with 4 mm in diameter, present in LS. The diameter of the tube is 23 mm. Hence, the LS–nitrogen contact area is 616.5 mm².

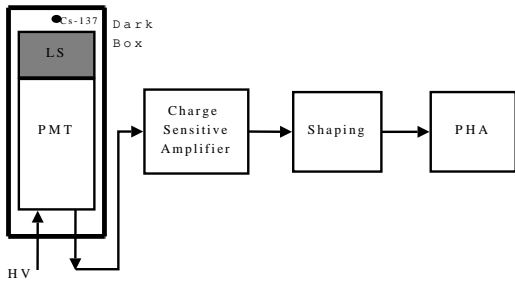


Fig. 2. Schematic view of the experimental setup.

The setup shown in Fig. 2 was used to measure the light output. LS was encapsulated in a cylindrical teflon cell (5 cm in diameter and 2.5 cm in height). The end of the cell was terminated with UV glass which was coupled to a 2-inch high energy resolution PMT (Hamamatsu CR105). The cell and PMT were placed in a dark steel box. The cell was exposed to a ¹³⁷Cs γ -ray source.

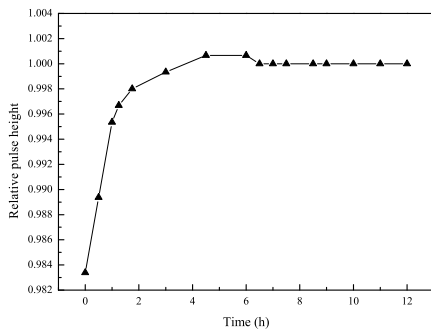


Fig. 3. System stability in 12 hours. The stability was tested by a LED driven by a pulse generator

The charge of PMT output pulse was firstly covered to amplitude by a charge sensitive amplifier and then shaped by shaping filter. Finally, the shaped signal amplitude was analyzed by a pulse height analyzer. System stability has been measured by means of a LED driven by pulser generator. Fig. 3 shows the system stability. System trended stable after 6 hours burning. System was burned about 12 hours before data acquisition in our experiment.

4 Data Analysis and Results

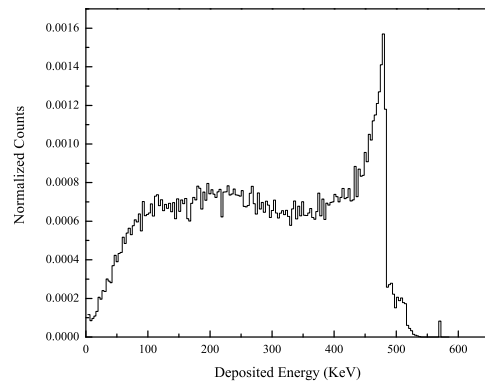


Fig. 4. Energy response of LS to the ¹³⁷Cs γ -ray source simulated by GRESP. The counts are normalized to the number of γ -rays emitted from the ¹³⁷Cs source.

Energy spectrum $N(E)$ of the Compton scattering electrons is generated by means of Monte Carlo GRESP code. Fig. 4 shows the simulation result. It should be noted that the resolution smearing is not considered in the GRESP Monte Carlo code. We considered the resolution smearing similar to the way described in Ref [9]. The “realistic” Monte Carlo spectrum can be obtained from the convolution of the simulation spectrum with the system response function,

$$N^{MC}(H) = \int R(H, L)N_L(L)dL, \quad (12)$$

where $R(H, L)$ is the response function, H is the ADC channel and $N_L(L)$ is the spectrum of light output. For electrons (above about 50 KeV), the light output L , the energy emitted as fluorescence, is proportional to the energy E deposited in the LS^[8], i.e.

$$L = SE, \quad (13)$$

where S is the absolute scintillation efficiency. The light output L can be defined to be in units such that it is equal to the electron energy E ^[10], i.e $S = 1$ and

$$L(E) = E. \quad (14)$$

When oxygen presents in LS, the light yield will decrease. Let the quenching factor, i.e. the light yield with the oxygen quenching to that without the oxygen quenching, I/I_0 , be f_Q . Then the light output can be rewritten as

$$L = f_Q E. \quad (15)$$

It should be reminded that f_Q is 1 for LS without a quencher. Considering that the spectrum of deposited energy is $N(E)$, the spectrum L , $N_L(L)$, is $N(L/f_Q S)/f_Q$. Assuming that the response $R(H, L)$ of the detector for the fixed light output is Gaussian,

$$R(H, L) = B \exp\left(-\frac{(H - cL)^2}{2\sigma_{cL}^2}\right), \quad (16)$$

where c is the light output to ADC channel conversion factor, and B is the normalization factor between the ‘‘realistic’’ Monte Carlo spectrum and the experimental spectrum. σ_{cL} can be expressed in the form of the system resolution,

$$\sigma_{cL} = \frac{cL}{2\sqrt{2\ln 2}}\rho, \quad (17)$$

where $\rho = \Delta(cL)/cL$ is the detector resolution, i.e. FWHM. and the background can be thought to be exponential^[6],

$$N^{BG}(H) = c_1 \exp(-c_2 H + c_3), \quad (18)$$

where c_1 , c_2 , c_3 are parameters of the background. Then, the expected experimental spectrum can be written as

$$N^{MC}(H) = B \int \exp\left(-\frac{(H - cf_Q E)}{2\sigma_E^2}\right) N(E) dE + c_1 \exp(-c_2 H + c_3), \quad (19)$$

with

$$\sigma_E = \frac{cf_Q E \rho}{2\sqrt{2\ln 2}}. \quad (20)$$

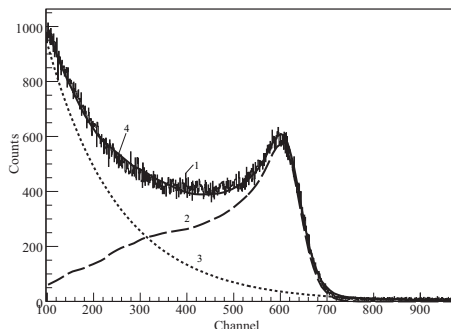


Fig. 5. (1) Experimental spectrum, (2) ‘‘realistic’’ Monte Carlo spectrum, (3) Background defined in Eq. (18), (4) expected experimental spectrum defined in Eq. (19) for ^{137}Cs .

The expected experimental spectrum is determined by B, c_1, c_2, c_3, c, f_Q and the detector resolution ρ . c depends on the optical properties of the cell, PMT and electronics. It is independent of quenching and can be treated as a constant in our experiment. Hence the item $f_Q c$, which is proportional to the quenching factor, can be taken as one free parameter. To evaluate the free parameters we used the ROOT package (CERN data analysis package) to fit the experimental spectrum with Eq. (19). Fig. 5 shows the fit result of the background, the realistic spectrum, and the expected spectrum for the experimental spectrum. The items $f_Q c$ for different LS samples can be obtained by fitting their experimental spectrums with Eq. (19). With the increase of the nitrogen bubbling time, the light output increased. We assume that oxygen was fully bubbled, namely no oxygen quenching effect remains in LS, when the light yield change little. It should be reminded that the quenching factor, I/I_0 , for full bubbled LS is 1. c was established from the fit result of the full bubbled LS. Then, the value of f_Q for different LS samples were determined. Fig. 6 shows the f_Q for six LS samples. The solid line in Fig. 6 shows the fits with Eq.(9). From the experimental result, we know that the light yield is increased by about 11% (20°C) by means of removing the oxygen in LS.

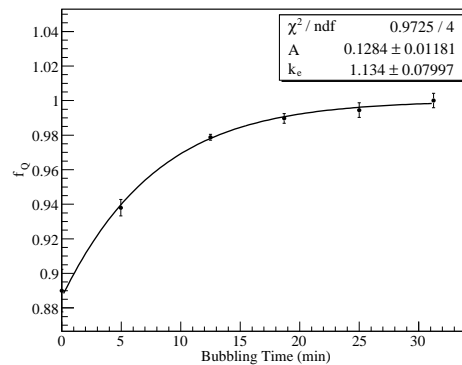


Fig. 6. f_Q as a function of the bubbling time. The solid curve shows the fits with Eq. (9).

5 Conclusions

The oxygen quenching in LAB liquid scintillator and the degassing model have been studied. From the experiment, we know that LAB LS light yield is increased by 11% by fully removing oxygen at 20°C. Moreover, we proposed a model to determine the relationship between the light yield and the bubbling time in this paper. The parameters in the model have been fixed experimentally.

6 Acknowledgements

This work is supported by the Natural Science Foundation of China (211202037). The authors would

like to thank Xin-Heng Guo, Jun Cao, Bing-Lin Yong and Xi-Chao Ruan and people from Institute of High Energy Physics who gave help and suggestion for our work.

References

- 1 F. Masetti et al. *J. Lumin.*, 1996, **68**(1): 15—25
- 2 G. Ranucci et al. *Nucl. Instr. and Meth. A*, 1998, **412**(2): 374—386
- 3 Y. Kino et al. *J. Nucl. Radiochem. Sci.*, 2000, **1**(2): 63—68
- 4 Terry L. Brewer, *J. Am. Chem. Soc.*, 1971, **93**(3): 775—776
- 5 D. J. Chleck, C. A. Ziegler. *Rev. Sci. Instrum.*, 1957, **28**: 466—467
- 6 LIU Jin-Chang et al. *HEP & NP*, 2007, **30**(1): 76—79 (in Chinese)
- 7 Y. Ding et al. *Nucl. Instr. and Meth. A*, 2008, **584**(1): 238—243
- 8 J. B. Birks. *The Theory and Practice of Scintillation Counting*. London: Pergamon Press, 1964. 185
- 9 F. Arneodo et al. *Nucl. Instr. and Meth. A*, 1998, **418**(2): 285—299
- 10 R.E. Pywell et al. *Nucl. Instr. and Meth. A*, 2006, **565**(2): 725—730